



Characterization of the Rate of Injection of Diesel Solenoid Injectors Operated in the Multiple Injection Strategy: A Comparison of the Spray Momentum and Bosch Tube Methods

OPEN ACCESS

Edited by:

Michael L. Traver,
Aramco Americas, United States

Reviewed by:

Joaquin De La Morena,
Polytechnic University of Valencia,
Spain

Bianca Maria Vaglieco,
CNR-Istituto di Scienze e Tecnologie
per l'Energia e la Mobilità Sostenibili
(STEMS), Italy

*Correspondence:

Moez Ben Houidi
moez.benhoudi@kaust.edu.sa

[†]These authors share first authorship

Specialty section:

This article was submitted to
Engine and Automotive Engineering,
a section of the journal
Frontiers in Mechanical Engineering

Received: 04 March 2022

Accepted: 13 June 2022

Published: 18 July 2022

Citation:

Aljohani BS, Ben Houidi M, Du J,
Dyuisenakhmetov A, Mohan B,
AlRamadan A and Roberts WL (2022)
Characterization of the Rate of Injection
of Diesel Solenoid Injectors Operated
in the Multiple Injection Strategy: A
Comparison of the Spray Momentum
and Bosch Tube Methods.
Front. Mech. Eng 8:889255.
doi: 10.3389/fmech.2022.889255

Bassam S. Aljohani^{1,2†}, Moez Ben Houidi^{1*†}, Jianguo Du^{1,3}, Aibolat Dyuisenakhmetov¹,
Balaji Mohan⁴, Abdullah AlRamadan⁴ and William L. Roberts¹

¹Clean Combustion Research Center, Physical Sciences and Engineering Division, King Abdullah University of Science and Technology (KAUST), Thuwal, Saudi Arabia, ²Thermofluids Laboratory, College of Engineering, Mechanical Engineering Department, Taibah University, Yanbu, Saudi Arabia, ³Foshan Xianhu Laboratory of the Advanced Energy Science and Technology Guangdong Laboratory, Xianhu Hydrogen Valley, Foshan, China, ⁴Transport Technologies R&D Division, Saudi Aramco Research & Development Center (R&DC), Dhahran, Saudi Arabia

Multiple injection strategies can be used for controlling the heat release rate in an engine, particularly in compression ignition engines. This can mitigate the heat transfer losses and overcome the limitation related to the maximum pressure allowed for a particular engine. Controlling heat release with repetitive injections requires precise characterization of the fuel injection rates. In such a configuration, the injector used should be characterized for its hydraulic delay, rate of injection, and the effect of dwell timing with multiple injections. This study investigates the fuel injection behavior of a high-flow-rate solenoid injector operated with single and double injections. Two characterization methods, the momentum flux, and the Bosch tube are used and compared to investigate their suitability with the multiple injection strategies. Experiments with single injection are conducted by varying the Energizing Timing (ET) from 0.5 up to 2 ms. The tests with multiple injections (i.e., double injections) are conducted with a fixed ET of 0.5 ms, while the dwell times (δt) are varied from 0.1 up to 1 ms. All tests are performed at 500, 1000, 1500, and 2000 bar rail pressures. Depending on the injection pressure, the injector's needle could not fully close with short dwell times and the injections are merged. The momentum flux method has faster ramp-up and decaying and more oscillations in the quasi-steady-state phase compared to the Bosch tube method. The effective duration of injection is overpredicted with the Bosch tube method. The momentum flux method is demonstrated to be more suitable for measuring the ROI of multiple injection strategies.

Keywords: rate of injection, multiple injections, spray, momentum flux, Bosch tube

1 INTRODUCTION

The substantial advancement in injection systems in the past decade has significantly contributed to improving the efficiency of compression ignition engines. With ultra-high-pressure injection systems and precise control of fuel injection, the engine-out emissions, such as soot, unburned hydrocarbons, carbon monoxide, and oxides of nitrogen (NO_x), were reduced to comply with stringent regulations. The state-of-the-art direct injection systems allow a large degree of flexibility to operate at ultra-high injection pressures and multiple repetitive injection pulses. This development facilitates controlling the fuel flow rate to shape the rate of heat release, which subsequently can improve engine efficiency and reduce emissions (Mohan et al., 2013; Lam et al., 2015; Cung et al., 2017; Bhavani Shankar et al., 2017; Lam et al., 2019; Al Ramadan et al., 2020; Harsh et al., 2020; Tang et al., 2020; Jin et al., 2021; Aljabri et al., 2022; Zhang et al., 2022). The multiple injection concept was explored to decouple the NO_x -soot trade-off, for instance, in the work of Nehmer and Reitz (1994), when operated at high injection pressure with split injections. It was then shown that NO_x emissions with a split injection schematic could be decreased because of the controllability of the rate of heat release (fuel staging) at which the main combustion started. Marginal soot levels were observed depending on the adapted injection strategy as the main combustion was more tilted toward the injection at which combustion was phased. In conventional diesel combustion, the soot formation at the spray tip with a single injection was diminished with split injection as this induced an improved fuel-air mixing (Nehmer and Reitz, 1994).

At high ambient density conditions, we have investigated the potential of employing multiple injections to achieve isobaric combustion using a heavy-duty D13 Volvo engine (Babayev et al., 2019). In the context of high-pressure combustion, isobaric combustion has the prospect of attaining high efficiency through increased compression ratio or ultra-high boosting. The peak cylinder pressure is constrained to not exceed the maximum allowed for this engine, which limited the operation with conventional diesel combustion (CDC). The study demonstrated the advantages of isobaric combustion in terms of efficiency and emissions compared to the single-injection strategy employed by CDC. Controlling the rate of heat release is critical for isobaric combustion, and this was demonstrated in our *in-situ* injection rate measurement studies (Aljohani et al., 2019; Babayev et al., 2019) where the staged injection was linked to the heat release shape.

The injection of fuel at ultra-high pressure is a complex process that is highly influenced by engine operating conditions in terms of fuel temperature, pressure, and the system layout (injector, rail, pipes, etc.). The injection generates pressure waves with large gradients that are reflected in the common rail and through the pipes and the injectors. These have a significant impact on the resultant rate of injection (ROI) (Catania et al., 2008; Manin et al., 2012; Payri et al., 2012; Mohan et al., 2018). When measuring the ROI, it is more accurate to reproduce as much as possible engine-like conditions (AlRamadan et al., 2019; Aljohani et al., 2019). The choice of

the ROI measurement methodology is critical, particularly for multiple injection schemes (Martínez-Martínez et al., 2021). For instance, the spray momentum method could not characterize the ROI of short early injections as demonstrated in AlRamadan et al. (2019). With split injections, the injector behavior was highly influenced by the dwell times as the hydraulic delays of the second injection were significantly shortened which led to injections' merging. This raises questions about the technical limitation of such a method for multiple injections with short injection pulses.

In the literature, several techniques have been proposed to characterize the ROI at high injection pressures. Despite the novelty and accuracy of each technique, Bosch tube, Zeuch, and momentum flux techniques have been well-validated with computational fluid dynamics. The Bosch tube method (BM) is a benchmark method to characterize the rate of injection at specific backpressure. Its principles involve a measurement of the pressure wave generated when fuel is injected into a measuring tube filled and held at constant pressure through a check valve near the end of the measuring tube (Bosch, 1967). The check valve reflects the generated pressure wave to induce a reflected pressure signal on the pressure sensor. This pressure sensor is usually enclosed in a fixture near the injector nozzle and measures the incident and reflected pressure waves during an injection event. Thus, the pressure profile and speed of sound are deduced to calculate the injected mass. The momentum flux technique measures the impinging spray plume momentum flux on a force transducer installed perpendicular to the injector's nozzle hole. Since the transducer is positioned at a distance from the injector nozzle to allow for the spray to develop during injection, the resulting momentum flux is proportional to the injection rate and employed to estimate the spray velocity at the injector nozzle exit based on nozzle geometry, discharge coefficient, and assumed fuel density (Naber and Siebers, 1996; Payri et al., 2005). Torelli et al. (2018) evaluated the flow variation from shot to shot using an X-ray technique and showed that the flow was consistent and repeatable, which demonstrates that the discharge coefficient can be assumed constant.

The Zeuch method is based on the pressure measurement principle similar to the Bosch tube method (Matsuoka et al., 1969). However, the Zeuch method records the pressure increase when fuel is injected into a constant volume chamber maintained at a pressure (i.e., p). This injected fuel increases the chamber pressure (becomes $p + dp$), and the resulting pressure increase is proportional to the bulk modulus of the fuel and can estimate the injection rate with the differential pressure. A comparison of the Bosch tube and Zeuch methods to characterize the ROI did not show any significant differences. Although a pronounced and steeper initial ramp-up was observed with the Zeuch method (Bower and Foster, 1991), it was later shown that the Bosch tube and Zeuch methods gave different average rates of injection (Arcoumanis and Baniasad, 1993). One of the disadvantages of the Zeuch method over Bosch is its limitation in implementing minimum backpressure due to cavitation (Takamura et al., 1992).

With multi-hole injectors, the variation in the injected fuel between nozzle holes slightly alters the average rate of injection profiles, as seen in Luo et al. (2014), Zhou et al. (2016), and Luo et al. (2018). The numerical validation against an experimental

dataset of multi-hole injectors was explored in Zeng et al. (2012) to understand the variation from one orifice to another. The study revealed large flow losses and their impact on the injection from the different holes. A macroscopic laser technique was implemented with numerical analysis, which allowed visualizing the dominating forces associated with the liquid-jet breakup of multi-hole injectors. Their results revealed that the inertial, viscous, surface tension, and aerodynamic forces (i.e., drag forces) are the major active forces on the sensing element for the Momentum flux method (Zeng et al., 2012). Luo et al. (2014) studied the injection rates using the momentum flux method (MFM) for a six-hole diesel injector and employed an adjustable stand to align the sensing element for each hole to the spray perpendicular direction. They demonstrated a minor degree of dependence on the fuel quantity with the outlet-target distance and the target angle at which the spray plume was impinging. However, with a 12 mm and larger outlet-target distance, a noticeable delay at the start of injection and a lower peak in the injection rate was observed. In this study (Luo et al., 2014), the spray to the target distance was fixed at the optimal distance to capture one spray plume emerging from one of the six nozzle holes of the injector without interference with the other emerging spray plumes. The discharge coefficient of the non-cavitation diesel injection nozzle was investigated with the MFM and shown to strongly correlate to the injection pressure, while the average discharge coefficients were not significantly influenced. Comparable results were theoretically obtained for the discharge coefficient and found to be in the range of 0.9 at high injection pressure (Desantes et al., 2016). The discharge coefficient variations from one hole to another were in the range of 0.8–0.9, as also shown by Zhou et al. (2016). The influence of physical properties on diesel injectors using three-dimensional modeling with diesel surrogates was compared to gasoline fuels in Torelli et al. (2017). The effect of cavitation during full needle lift was less pronounced with diesel than the other tested fuels, and that cavitation is consistent with the discharge coefficient value chosen for this study. Thus, in the current work, a constant discharge coefficient value was considered to estimate the velocity at the injector nozzle outlet. The detailed velocity estimation is described in the later “Data Post-Processing” subsection.

Ge et al. (2019) used a CFD model to predict the initial liquid penetration length with a rate of injection measured by Zeuch and momentum flux measurement techniques. The ROI profile measured by the momentum flux method led to a faster rate of increase during the initial ramp-up compared to the initial ramp-up profile measured by the Zeuch method. Consistent results were obtained with liquid penetration length when using the ROI profile generated with the MFM. The velocity profiles from these two ROI profiles were used as an input to predict the liquid penetration length and compared to the measured penetration length. The simulation showed that the velocity profile generated from the MFM can predict the simulated data and was more consistent than simulations obtained from velocity profiles through the Zeuch ROI profile.

In this study, we investigate two well-validated ROI measurement techniques, momentum flux and Bosch tube

methods, to characterize a multi-hole diesel solenoid injector operated at single and double injection strategies with noticeably short dwell timings. This article is divided into three main sections. First, the experimental configuration and the post-processing are described for the momentum flux and Bosch tube methods. Second, a brief review of the theoretical background of these methods is presented. Finally, the experimental results from the current study are presented and the differences between BM and MFM are demonstrated and discussed.

2 EXPERIMENTAL SETUP AND TEST BENCH

One common test bench was utilized to acquire the injection rate measurements for the momentum flux and Bosch tube methods. The test bench was flexible and allowed rapid conversion from one configuration to the other.

2.1 Fuel Injection System

The fuel injection system was composed of: a fuel tank, a low-pressure pump, a fuel filter, a high-pressure (up to 3000 bar) air-driven pneumatic pump, a truck-size diesel common rail, a six-hole F2 Delphi injector (Meek et al., 2014), and a backpressure regulator to control the pressure in the return line. The layout of these components is described in **Figure 1**. The injection circuit was reproducing the on-engine conditions as the in-series rail and high-pressure (HP) pipes are used. The fuel used for this study was a commercial diesel fuel with a density of 835kg/m^3 and kinematic viscosity of $2.43\text{mm}^2/\text{s}$. **Table 1** shows the fuel's properties.

2.2 Momentum Flux Measurement

In the MFM, a piezoelectric pressure sensor (AVL GU22C, used as a force sensor) was positioned in front of one of the injector holes at a distance of 4 mm from the nozzle, as illustrated in **Figure 1**. A container was used to collect the total mass of fuel injected over a sufficiently high number of tests. Thus, the average ROI could be calibrated against the injected mass per test (cycle). A Kistler 5051A charge amplifier was used to amplify the sensor's signal while applying a low-pass hardware filter at 6 kHz. It is worth noting that the natural frequency of the sensor is 100 kHz and the filter applied was aimed to remove the force fluctuation induced by the spray impingement on the sensing element. We found that the fluctuation frequency is consistent with the natural frequency of the sensor. A National Instruments CompactRIO system was used to drive the injector and to record the measured signals at a sampling rate of 500 kHz in a well-synchronized manner.

2.3 Bosch Tube Measurement

The test rig used in MFM was adapted to include the arrangement for the Bosch tube method. The part holding the piezoelectric pressure sensor in front of the injector nozzle was replaced with a new part holding another pressure transducer mounted vertically to the fuel channel (see illustration in **Figure 1**). The same

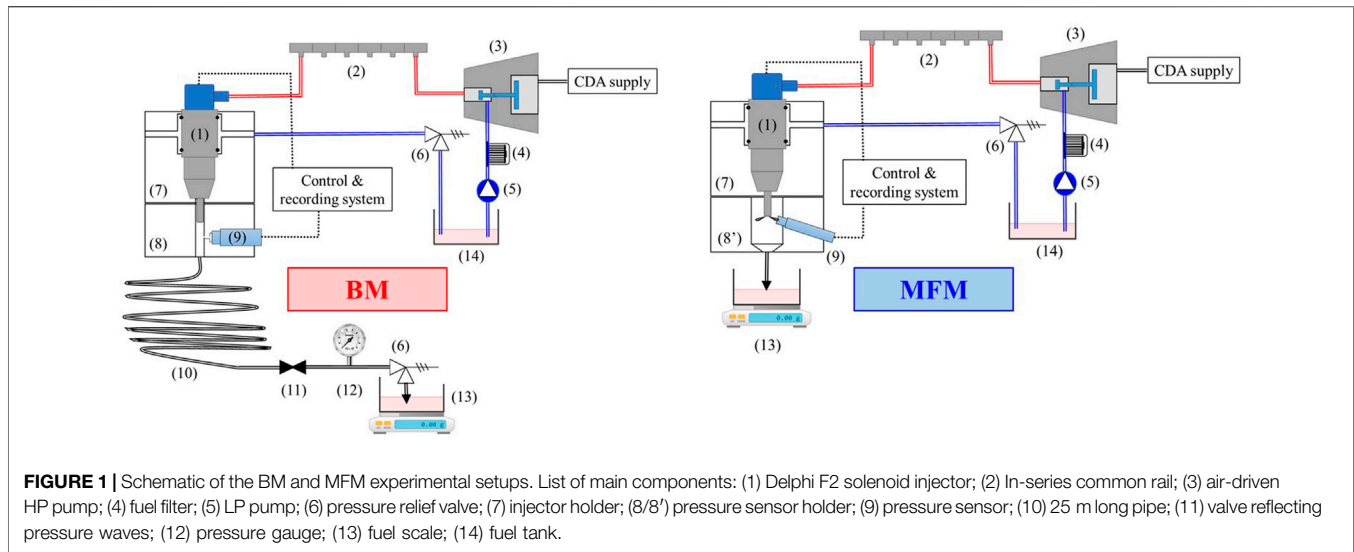


TABLE 1 | Properties of the certified diesel fuel used in current ROI measurements.

Cetane number	53.8
Density at 15 degC	835.1 kg/m ³
Viscosity at 40 degC	2.437 mm ² /s
Carbon content	86.98 %m/m
Hydrogen content	13.02 %m/m
Lower Heating Value (LHV)	43.21 MJ/kg

injection system (drive, rail, piping, etc.), charge amplifier, and acquisition were used in the BM. The same signal filtration methods were also employed. The fuel channel enclosing the injector nozzle tip was 7.2 mm in diameter and 7 mm in length. The measuring tube (25 m in length) was mounted at the extremity of the fuel channel and had an inner diameter of 3.9 mm. A valve was mounted at the end of the measuring tube to reflect the pressure wave and a relief valve was used to regulate the backpressure at 4 bar. The effect of different backpressure levels has been investigated at a reference condition of 1500 bar injection pressure. The injected mass was compared with engine fuel consumption experiments and the differences observed were within the test-to-test variation. This assumption on the effect of backpressure holds as long as the injection pressure is significantly higher than the backpressure considered in the target application on engines.

3 THEORETICAL BACKGROUND AND METHODOLOGY

In general, the mass conservation equation is applied to quantify the mass flow rate. The density variation of the injected liquid is usually deemed negligible and density is assumed constant as the ambient bulk temperature and pressure are maintained close to the standard conditions ($T_{\infty} = 298.15^{\circ}\text{C}$ and pressure

$p_{\infty} = 1\text{atm}$). This assumption leads to the following form of the integral mass conservation equation:

$$\dot{m}(t) = \int \rho_f u_{eff} dA, \quad (1)$$

where ρ_f is the fuel density and u_{eff} is the velocity at the nozzle outlet of the liquid spray plume.

The nozzle outlet velocity accounts for the liquid phase assuming a non-evaporating diesel spray configuration. To estimate the velocity of the spray plume, Bosch tube and momentum flux methods apply different measuring principles.

3.1 Bosch Tube Method

In the Bosch tube measurement, the determination of an incremental fuel quantity is based on the pressure-velocity equation derived from the hydraulic pulse theorem assuming a single pressure wave in a flow field. The pressure waves in a fluid propagate at the speed of sound. Assuming a uniform one-dimensional fluid flow, the hydraulic pulse theorem allows a good estimation of the fluid flow rate. The ROI equation is estimated according to the work of Bosch (1967) as

$$\dot{m}(t) = \frac{A}{a(t)} p(t), \quad (2)$$

where A is the fixture cross-sectional area, $a(t)$ is the speed of sound of a pressure wave, and $p(t)$ is the corrected pressure signal.

In the current work, the speed of sound was measured for each test case by recording the delay between the incident pressure wave (defining the ROI) and its reflection on the valve installed at the end of the long tube. This substituted the need to use a diesel surrogate fuel with a well-known speed of sound characteristics. The speed of sound measurement was consistent throughout the entire test matrix as its standard deviation was lower than 1.5%. The cross-sectional area was calculated considering the average of the fuel channel and measuring tube inner diameters. The quantitative ROI was corrected based on a calibration approach as described in the later post-processing section.

The Bosch method theory is appropriate for a single uniform pressure wave traveling at the speed of sound. This raises questions about the adequacy of such an approach to characterize the ROI of multiple injections. The current work addresses this issue by comparing the BM with MFM in a split injection scheme where the dwell time was varied.

3.2 Momentum Flux Method

The momentum flux method involves the measurement of the momentum flux produced by the spray plume impingement on a force-sensing element. The liquid fuel injection undergoes physical flow restrictions and boundary conditions that induce complex phenomena such as cavitation, and pressure drop. To simplify the momentum flux modeling, the spray plumes developed ahead of the injector nozzle holes were assumed to be in a liquid phase with constant density. Also, an effective area and velocity were assumed, which simplified the definition of flow coefficients as reported in Payri et al. (2005). The spray momentum is denoted in the following form:

$$\dot{M}(t) = \int \rho_f u_{eff}^2 dA. \quad (3)$$

Based on the conservation of momentum, the momentum equation can be considered in the form of the spray momentum flux equivalent to the spray force exerted upstream on the target sensing area of a force sensor. Hence, the momentum equation is denoted as

$$\dot{M}(t) = F. \quad (4)$$

With Eqs. 2, 3, 4, the mass flow rate can, therefore, be treated as proportional to the spray momentum flux as follows:

$$\dot{m}(t) \sim \sqrt{F(t)}, \quad (5)$$

where $F(t)$ is the spray momentum force exerted on the sensor.

The injection rate can be obtained quantitatively by two methods: 1) measurement of the force with a calibrated sensor and determining the proportional factors based on the fuel density, and the effective nozzle hole area, or 2) measure the force to get the ROI shape and apply a calibration based on the weighting of the total injected fuel. In the current study, the second option was used to get the quantitative ROI measurement.

3.3 Data Post-Processing

In addition to the hardware filtration, an FIR low-pass filter with a threshold of 4 kHz was applied to the raw signals. The pressure and force profiles were pegged and corrected for the charge leak compensation. More details about this post-processing were reported in (Aljohani et al., 2019). The signals were then corrected for minor noise fluctuations at the reference levels and averaged over the cycles (tests) recorded in each specific case. In the BM, 5 cycles have been considered for the averaging, while 30 cycles have been considered for the MFM measurements. This was motivated by the low cycle-to-cycle variation observed in the BM compared to the MFM configuration.

In the momentum flux method, it was essential to account for the time required for the spray plume to travel from the nozzle hole to the sensor membrane, located at 4 mm from the injector nozzle hole. The spray plume velocity at the nozzle hole was estimated based on the injection rate, fuel density, number of nozzle holes, their area, and assumed discharge coefficient. The following equation was used to account for the spray velocity:

$$v(t) = \frac{\dot{m}(t)}{N_h \rho_f A_h C_d}, \quad (6)$$

where $\dot{m}(t)$ is the injection rate obtained by the Momentum flux method, N_h is the number of holes, ρ_f is the fuel density, A_h is the cross-sectional area of the nozzle hole, and C_d is the discharge coefficient.

The discharge coefficient considered was 0.9 and this was based on information provided by the injector manufacturer (the injector used had a k factor of 3). This estimation is consistent with typical high-pressure diesel injectors (Desantes et al., 2016; Zhou et al., 2016). Consequently, the velocity was integrated over time to obtain a definite distance between the nozzle holes and the plume edge. Since the velocity profile is a function of the injection rates, the travel time was calculated for each test case. The time required for the spray plume to travel from the nozzle hole to the sensor membrane was faster with higher injection pressures. This traveling delay is implemented to shift the signals of the momentum flux method to correct the hydraulic delays. The start of injection hydraulic delay was defined as the time interval between the start of the injector's energizing and the time at which a plume is issued from the nozzle holes (often described as the effective start of injection).

In the BM, there was a minor need for hydraulic delay correction. The pressure waves' travel time between the injector nozzle and the sensor located at 22 mm was approximately 12 μ s. This was four times lower than the typical hydraulic delay correction applied in the MFM. However, we had to correct the tail shape of the raw signal in the BM, as illustrated in Figure 2. It is well-known that the end of injection is driven by the injector's needle closing. Thus, the ROI is expected to be decreasing linearly at the end of injection. The tail shape of the BM raw measurement signal is caused by interference with transverse acoustic waves.

A calibration method was used to convert the qualitative ROI from MFM into a quantitative measurement. At least 6 g of fuel have been collected from a defined number of injections in each tested case. This defined the injected mass per stroke, which was used to calibrate the average ROI profiles. The same calibration was used to calculate a correction factor for the Bosch tube method. The final ROI measurements were based on the most accurate calibrations, which corresponded to an average correction factor of 1.14.

The test matrix in the current work is summarized below in Table 2. In the double injections cases, the same post-processing algorithms were applied, and minor adjustments were needed to allow the proper correction of the ROI profiles measured with BM.

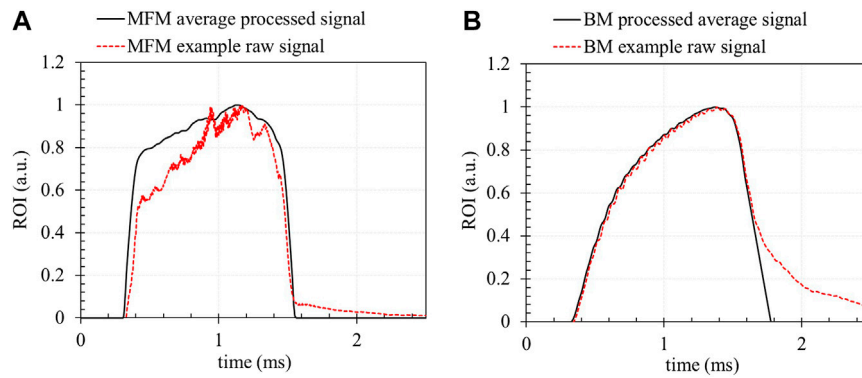


FIGURE 2 | Illustration of an example raw signal compared to the post-processed average ROI [(A) momentum flux method MFM. (B) Bosch tube method BM]. Conditions: injection pressure 1500 bar; duration of injection (DOI) 1 ms.

TABLE 2 | Summary of the test conditions for single and double injections performed with both MFM and BM.

Injection configuration	Single	Split/double
Rail pressure (bar)	500, 1000, 1500, 2000	
DOI or Dwell time (ms)	0.5, 0.8, 1, 1.6, 2	1, 0.5, 0.4, 0.3, 0.2, 0.1

4 RESULTS AND DISCUSSION

4.1 Measurement Uncertainties

4.1.1 Cyclic Variability

The cyclic variabilities of the ROI measurements have been assessed by calculating the standard deviation (STD) of the injected fuel mass from each method (BM and MFM) throughout the entire test conditions. The results are presented in **Figure 3**. In general, the BM had a very low cyclic variability that did not depend on the injection pressure level. However, the MFM had a higher cycle-to-cycle variation and this was even larger with low injected quantities. The STD of the injected fuel mass was higher at lower injection pressure and smaller duration of injection (DOI). In split/double injection, the effect of the injection pressure on the ROI measured with MFM was also significant as the higher injection pressure cases had

lower cyclic variability. With smaller dwell times, the STD of the injected mass with MFM decreased, and this is also correlated to the increased injected mass caused by the merging of the injections (see the later section reporting the comparison of the ROIs of BM and MFM). The higher cyclic variability with MFM was mainly caused by the ROI variability from plume to plume. In the current study, a six-hole injector was characterized and a single force sensor was installed in front of one of the plumes. On the other hand, the BM was not affected by the plume-to-plume variability as the measured pressure wave downstream of the injector was resulting from the fuel injected from all the nozzle holes.

4.1.2 Hydraulic Delays

The injection hydraulic delays were defined as the time lapses between the energizing timing (ET) and the effective injection of fuel, known as the positive ROI. The start of injection (SOI) hydraulic delay corresponds to the time lapse between the start of the injection current applied to the injector solenoid valve and the instant at which the first liquid fuels are ejected from the nozzle holes. The end of injection (EOI) hydraulic delay corresponds to the time lapse between the end of the ET and the effective end of injection. The hydraulic delay results are presented in **Figure 4**. For both BM and MFM, the SOI hydraulic delay was mainly

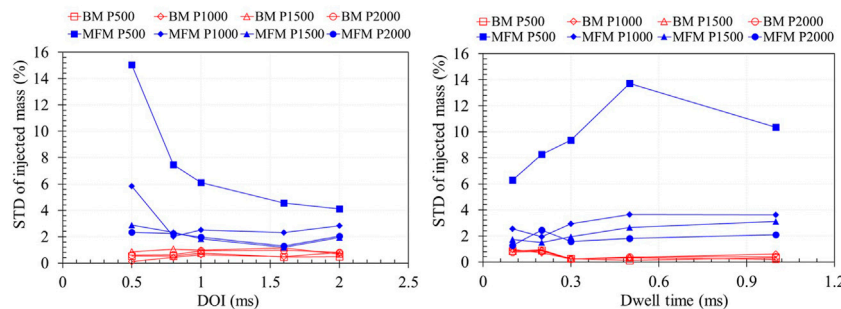


FIGURE 3 | Comparison of the cyclic variabilities of BM and MFM observed at different injection pressures, DOI, and Dwell times for the split injection tests.

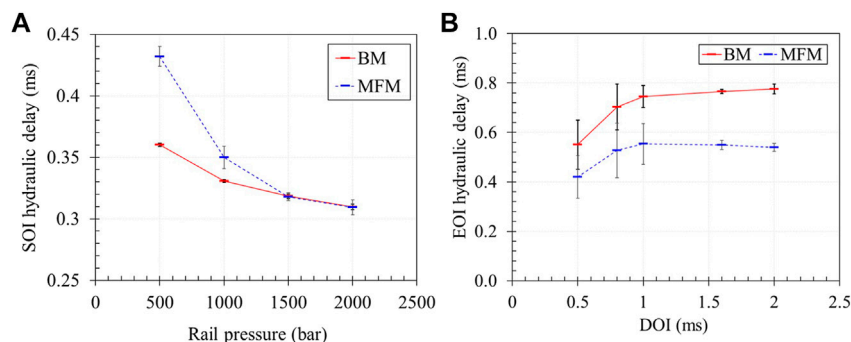


FIGURE 4 | Comparison of the calculated hydraulic delays from BM and MFM; **(A)** at different injection pressures; **(B)** at different DOI.

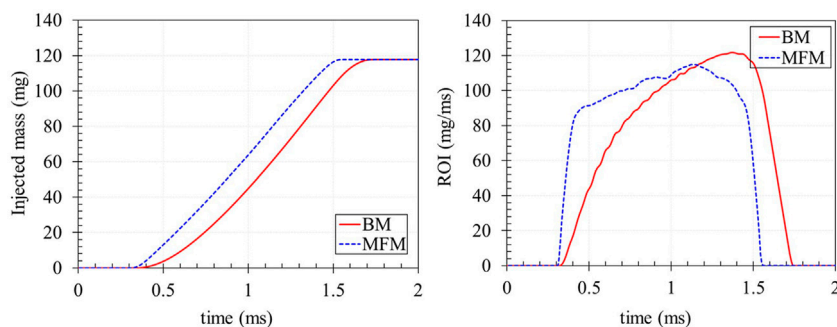


FIGURE 5 | Average Rate of Injection from BM and MFM at 1500 bar injection pressure and a DOI of 1 ms.

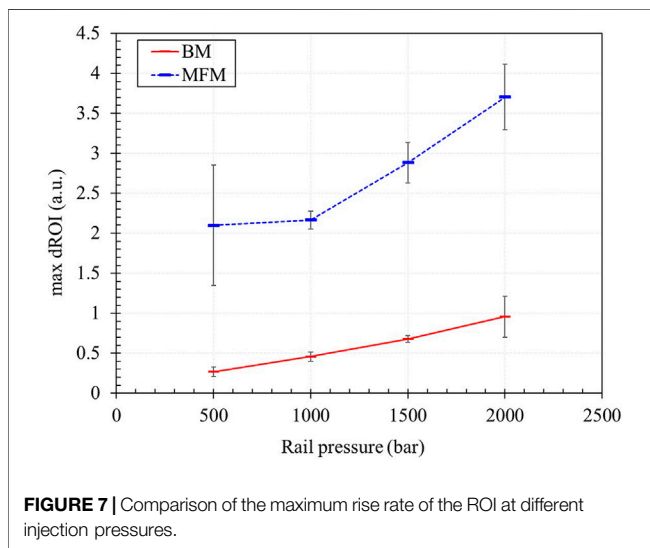
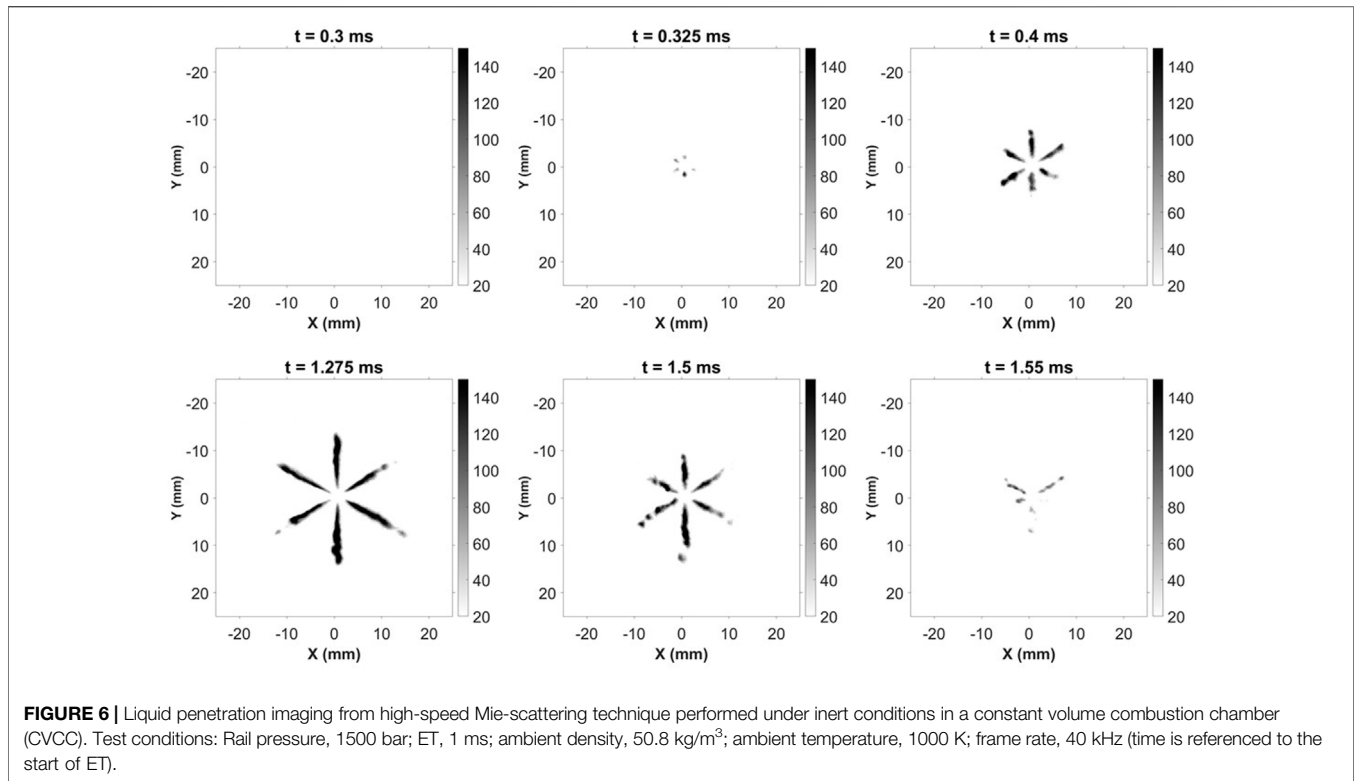
influenced by the injection pressure whereas the EOI hydraulic delay was rather influenced by the DOI. The SOI hydraulic delays of BM and MFM were consistent at high injection pressures, while they had significant deviation at pressures below 1000 bar. This demonstrated the adequacy of the correction applied in the post-processing, particularly at high injection pressures. At lower rail pressures, the SOI hydraulic delays of the MFM had a higher cyclic variation which demonstrated the limitation of this method at low injection pressures and small injected quantities. Under such conditions, the measurement of the spray momentum is challenging as it becomes highly influenced by the shape of the spray plume and the position of the force sensor. Overall, the EOI hydraulic delay with BM was consistently higher than that with MFM (approximately 0.2 ms longer). Thus, under identical injection control conditions, the DOI measured with BM was longer than that measured with MFM. The EOI hydraulic delays of BM and MFM were consistently constant and stable at ETs above 1 ms. At shorter injection durations, the cyclic variabilities were significantly higher and the average delays increased with increased ET. This is likely explained by the injector's needle opening dynamics. It seems that the needle reaches the fully open position at ETs above 1 ms.

4.1.3 Duration of Injection

In this section, the discrepancies in the ROI shapes of BM and MFM are investigated. In **Figure 5**, the ROI and the cumulative

injected mass of BM and MFM are compared at the reference condition of 1500 bar injection pressure and 1 ms ET. It is demonstrated that the ROI of the MFM had a steeper increase at the SOI and a steeper decrease at the EOI, compared to the BM. As demonstrated in the previous section, the effective DOI measured with MFM was shorter. High-speed Mie-scattering technique was performed to measure the effective hydraulic delay and DOI at the above reference condition with a time resolution of 25 μ s. A selection of these images at the SOI and EOI is presented in **Figure 6**. The images provided a qualitative assessment of the liquid phase at these instants. This illustrated the differences in shape from one plume to another. The results also demonstrated that the SOI hydraulic delay is properly measured with both methods at the rail pressure of 1500 bar. However, the EOI hydraulic delay and DOI of the MFM are more consistent with the visualization technique, as the BM overpredicted the DOI.

The maximum rise rate of the ROI measured with BM and MFM are compared at different injection pressures in **Figure 7**. This illustrates the differences in the ROI shape at the SOI and demonstrated the sensitivity of the ROI to the rail pressure increase. It can be concluded that both methods are capable of detecting the faster ROI at the SOI resulting from the increased injection pressure. However, the MFM demonstrated a higher sensitivity to the rail pressure variation. It is important to highlight that the ROI



measured with BM is based on a pressure wave measurement downstream of the injector nozzle. The pressure wave considered in the calculation is not corrected for the potential significant wave dispersion and attenuation effects. The injection event might have generated shock waves causing interactions and attenuation through reflections in the transverse direction. Considering these phenomena and our above results, it can be concluded that the effective ROI is rather similar in shape to the one measured with MFM. This is

consistent with Ge et al. work (Ge et al., 2019) in which the authors demonstrated that the ROI measured with MFM is more suitable for consideration in CFD simulations. It has also been demonstrated in Bower and Foster (1991) that the ROI measured with the Zeuch method had a pronounced and steeper initial ramp-up compared to BM.

It is worth highlighting that, according to BM measurement, the quantity of fuel injected at the hydraulic delay correction time of MFM was lower than 0.18% of the total injected mass at the reference condition shown in **Figure 5**. At the same instant (approximately 0.05 ms after the effective SOI), the accumulated mass, according to the MFM, is approximately 1.9% of the total injected mass. Thus, any potential mass accumulation effect cannot explain the significant difference in the ROI shape at the SOI.

4.2 Single Injection

Single injections with ET from 0.5 to 2 ms were performed and the ROI was measured based on BM and MFM at rail pressures from 500 up to 2000 bar. The results are summarized and presented in **Figure 8**. The results confirmed that the differences in the ROI shape between the BM and the MFM are observed in all rail pressure and DOI investigated cases. In general, the MFM showed a more dynamic ROI with oscillations particularly pronounced at high injection pressures and reached a peak at approximately 1.2 ms after the start of energizing the injector valve. The ROI measured with BM has a significantly lower level of fluctuations and reached a

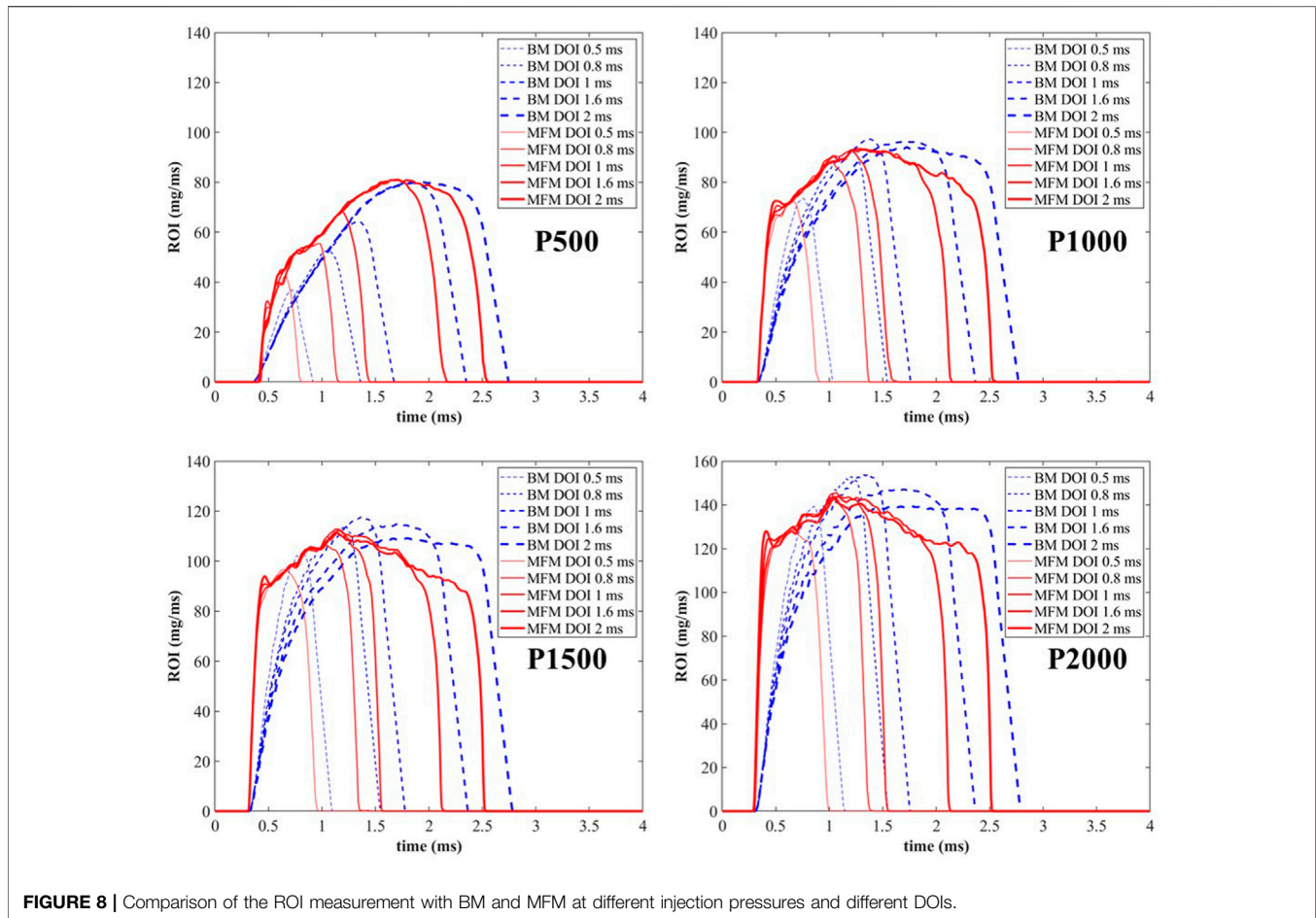


FIGURE 8 | Comparison of the ROI measurement with BM and MFM at different injection pressures and different DOIs.

plateau at approximately 1.5 ms after the start of energizing. The peak of the ROI is likely to indicate the instant at which the injector needle is fully opened, while the decay after the peak is explained by the pressure drop in the rail. The pressure drop was particularly significant at rail pressures above 500 bar and it ranged between 50 bar (at a rail pressure of 500 bar and a DOI of 2 ms) and 155 bar (at a rail pressure of 2000 bar and a DOI of 2 ms). It has been verified that the pressure drop is a phenomenon observed similarly in single-cylinder engine experiments in which the same in-series rail and high-pressure pipes were used.

The ROI measured with BM did not show a similar trend as the DOI was increased, particularly at the rail pressures of 1000, 1500, and 2000 bar. The ROI peaks of long injection cases were lower than those of shorter injections. This is likely explained by the dispersion and attenuation effects that are not corrected in the current BM.

4.3 Double Injection

The double/split injection strategy studied in the current study aimed to investigate the impact of short dwell times on the ROI. The DOI of each injection was fixed at a value representative of multiple injection strategies used in other

related engine research works (Al Ramadan et al., 2020; Harsh et al., 2020; Tang et al., 2020). The same injection system has been used in both current and previous studies. The ROI measurements with BM and MFM are compared at different injection pressures and dwell times in **Figure 9**. Although the dwell time was kept constant for both methods, the measured ROI profiles were substantially different. As highlighted in the previous section, the ROI measured with MFM was more dynamic as it had a faster ramp-up and decay phases. As the injection pressure was increased and the dwell time was decreased the split injections were merged. In such conditions, the injector's needle did not reach the fully closed position as its solenoid valve was still energized. It is demonstrated in **Figure 9** that the BM over-predicts the injection merging, which confirms that this method is not suitable for the characterization of multiple injections. Two phenomena may explain this: 1) the dispersion and damping of the pressure waves downstream of the injector nozzle, this has been identified and discussed in previous sections; 2) the pressure waves' interaction as the first incident wave is reflected on the pressure sensor. It is demonstrated in **Figure 9** that the injected mass from the second pulse is higher than that of the first in all the studied cases,

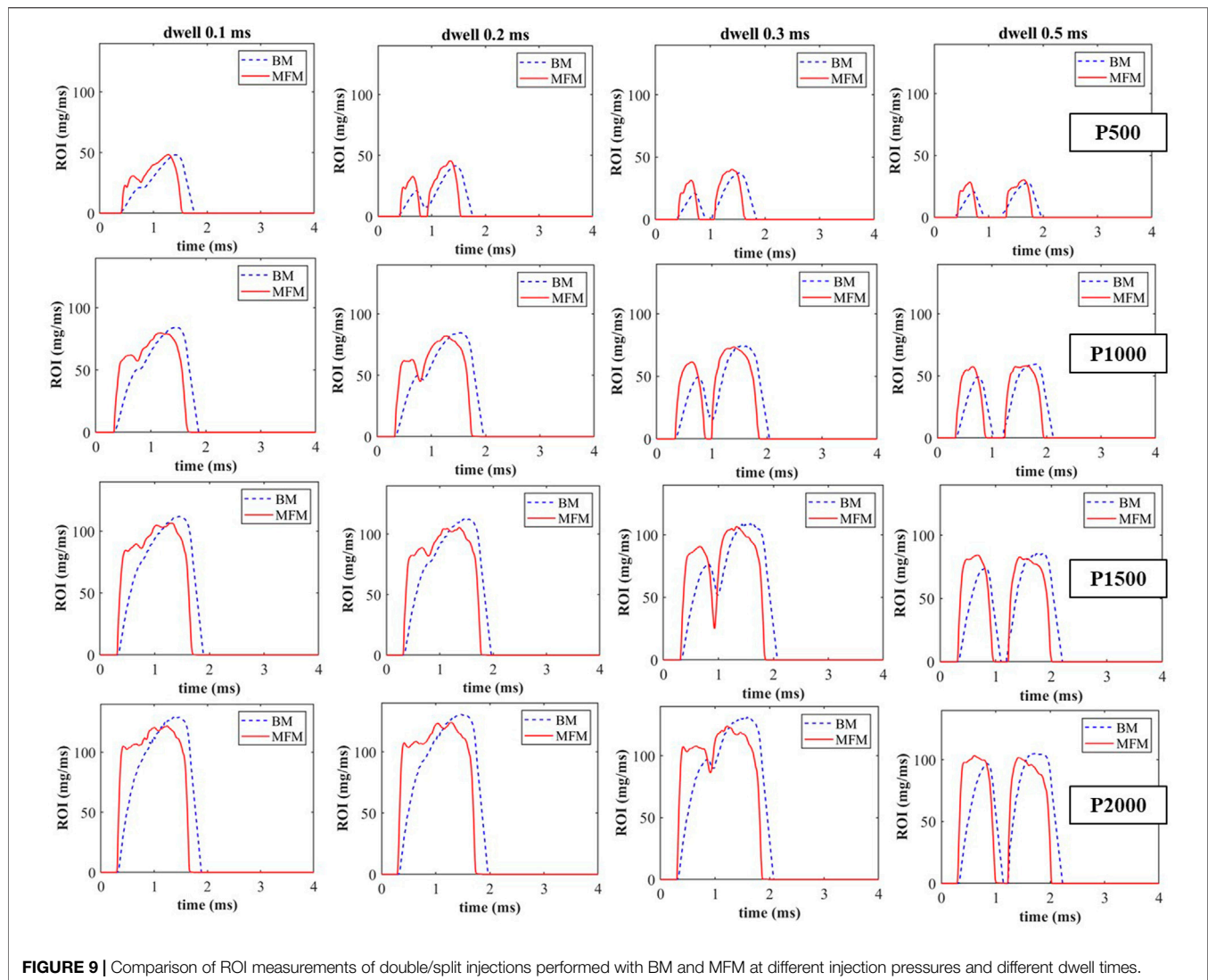


FIGURE 9 | Comparison of ROI measurements of double/split injections performed with BM and MFM at different injection pressures and different dwell times.

particularly at the dwell time of 0.5 ms where the MFM showed equally distributed quantities between the first and second injection.

5 CONCLUDING REMARKS

Single and multiple injection strategies were investigated and evaluated through a detailed examination of the rate of injection profiles measured with two methods: momentum flux and Bosch tube. The ET was varied with the single injection strategy from 0.5 to 2 ms. The multiple injections strategy focused on the effect of dwell time on the ROI profile at a constant energizing time for two consecutive injections. These split/double injections were performed at a fixed ET of 0.5 ms, whereas the dwell times ranged between 1 and 0.1 ms. All tests have been conducted with 500 up to 2000 bar injection pressures. High-speed Mie-scattering imaging technique was performed to investigate the effective

hydraulic delays and DOI at a reference condition (rail pressure of 1500 bar and T of 1 ms). The following concluding remarks can be drawn:

- The ROI measurement with BM had a lower cyclic variability compared to the MFM.
- The SOI hydraulic delays are better predicted with BM, which seemed more suitable for the ROI characterization of short injections and in general low injected quantities.
- The BM overpredicted the DOI as it seemed affected by the pressure wave dispersion and attenuation downstream of the injector nozzle.
- The ROI measurement with MFM showed a more dynamic behavior with, particularly, a steeper increase and decay at the SOI and EOI phases.
- The MFM is demonstrated to be more suitable for characterizing split injection strategies as the BM results are affected by acoustic effects resulting from pressure wave interactions.

- Although the ROI measurement with MFM showed a higher cycle-to-cycle variability, particularly with small injected quantities, their average profile seems to better reflect the effective ROI. The MFM seems to provide more realistic ROI profiles which would be more suitable for consideration in CFD simulations.

The current work has highlighted the pros and cons of using BM and MFM for the characterization of ROI of high-pressure liquid injectors. It opened perspectives for future works to rectify the BM setup and correct for the pressure wave dispersion and attenuation effects that have been demonstrated in this study. In future work, simulations will be conducted to investigate and compare the ROI profiles measured with BM and MFM.

DATA AVAILABILITY STATEMENT

The original contributions presented in the study are included in the article/Supplementary Material; further inquiries can be directed to the corresponding author.

AUTHOR CONTRIBUTIONS

MBH, BA, JD, and AD contributed to the conception, design, and building of the experimental setup. BA, MBH, and JD performed the experiments. MBH and BA performed the post-processing

REFERENCES

- Al Ramadan, A., Nyrenstedt, G., Ben Houidi, M., and Johansson, B. (2020). *Optical Diagnostics of Isooctane and N-Heptane Isobaric Combustion*. SAE Technical Paper. doi:10.4271/2020-01-1126
- Aljabri, H., Liu, X., Al-lehaibi, M., Cabezas, K. M., AlRamadan, A. S., Badra, J., et al. (2022). Fuel Flexibility Potential for Isobaric Combustion in a Compression Ignition Engine: A Computational Study. *Fuel* 316, 123281. doi:10.1016/j.fuel.2022.123281
- Aljohani, B., Ben Houidi, M., Babayev, R., Aljohani, K., and Johansson, B. (2019). In Situ Injection Rate Measurement to Study Single and Split Injections in a Heavy-Duty Diesel Engine. SAE Technical Paper. doi:10.4271/2019-24-0136
- AlRamadan, A., Ben Houidi, M., Aljohani, B. S., Eid, H., and Johansson, B. (2019). Compression Ratio and Intake Air Temperature Effect on the Fuel Flexibility of Compression Ignition Engine. *SAE Int. J. Adv. Curr. Prac. Mobil.* 2, 623–637. doi:10.4271/2019-24-0110
- Arcoumanis, C., and Baniasad, M. (1993). *Analysis of Consecutive Fuel Injection Rate Signals Obtained by the Zeuch and Bosch Methods*. SAE Technical Paper. doi:10.4271/930921
- Babayev, R., Houidi, M. B., Shankar, V., Aljohani, B., and Johansson, B. (2019). "Injection Strategies for Isobaric Combustion," in Proceeding of the 2019 JSAE/SAE Powertrains, Fuels and Lubricants, December 2019.
- Bhavani Shankar, V., Lam, N., Andersson, A., and Johansson, B. (2017). *Optimum Heat Release Rates for a Double Compression Expansion (DCEE) Engine*. SAE Technical Papers. doi:10.4271/2017-01-0636
- Bosch, W. (1967). *The Fuel Rate Indicator: A New Measuring Instrument for Display of the Characteristics of Individual Injection*. SAE Transactions, 641–662.
- Bower, G., and Foster, D. (1991). *A Comparison of the Bosch and Zuech Rate of Injection Meters*. SAE Technical Paper. doi:10.4271/910724

and the data analysis. BA and MBH wrote the first draft manuscript. WLR, BM, and AAR contributed to the conceptualization, and the review/approval of the manuscript.

FUNDING

This work was supported by the Saudi Aramco Research and Development Center under the FUELCOM program (Master Research Agreement Number 6600024505/01). This work was also supported by the King Abdullah University of Science and Technology (KAUST) Clean Combustion Research Center (CCRC) Center Competitive Fund (CCF).

ACKNOWLEDGMENTS

This study is based on the work supported by the Saudi Aramco Research and Development Center FUELCOM program under Master Research Agreement Number 6600024505/01. FUELCOM (Fuel Combustion for Advanced Engines) is a collaborative research undertaken between Saudi Aramco and KAUST intended to address the fundamental aspects of hydrocarbon fuel combustion in engines and develop fuel/engine design tools suitable for advanced combustion modes. This study is based on the work supported by the KAUST-CCRC Center Competitive Fund (CCF). The authors thank Cristian Avila Jimenez for his help with designing parts for the experimental setup.

- Catania, A. E., Ferrari, A., Manno, M., and Spessa, E. (2008). Experimental Investigation of Dynamics Effects on Multiple-Injection Common Rail System Performance. *J. Eng. Gas Turbines Power* 130, 032806. doi:10.1115/1.2835353
- Cung, K. D., Ciatti, S. A., Tanov, S., and Andersson, Ö. (2017). Low-temperature Combustion of High Octane Fuels in a Gasoline Compression Ignition Engine. *Front. Mech. Eng.* 3, 22. doi:10.3389/fmech.2017.00022
- Desantes, J. M., López, J. J., Carreres, M., and López-Pintor, D. (2016). Characterization and Prediction of the Discharge Coefficient of Non-cavitating Diesel Injection Nozzles. *Fuel* 184, 371–381. doi:10.1016/j.fuel.2016.07.026
- Ge, H., Johnson, J. E., Krishnamoorthy, H., Lee, S.-Y., Naber, J. D., Robarge, N., et al. (2019). A Comparison of Computational Fluid Dynamics Predicted Initial Liquid Penetration Using Rate of Injection Profiles Generated Using Two Different Measurement Techniques. *Int. J. Engine Res.* 20, 226–235. doi:10.1177/1468087417746475
- Harsh, G., Dyuisenakhmetov, A., Ben Houidi, M., Johansson, B., Badra, J., Cenker, E., et al. (2020). The Effect of Engine Speed, Exhaust Gas Recirculation, and Compression Ratio on Isobaric Combustion. *SAE Int. J. Engines* 13 (5), 603–16.
- Jin, Y., Wu, Q., Zhai, C., Kim, J., Luo, H.-l., Ogata, Y., et al. (2021). Evaporating Characteristics of Diesel Sprays under Split-Injection Condition with a Negative Dwell Time. *Energ. Mater. Front.* 2, 265–271. doi:10.1016/j.enmf.2021.08.003
- Lam, N., Tuner, M., Tunestal, P., Andersson, A., Lundgren, S., and Johansson, B. (2015). Double Compression Expansion Engine Concepts: a Path to High Efficiency. *SAE Int. J. Engines* 8, 1562–1578. doi:10.4271/2015-01-1260
- Lam, N., Tunestal, P., and Andersson, A. (2019). *Simulation of System Brake Efficiency in a Double Compression-Expansion Engine-Concept (DCEE) Based on Experimental Combustion Data*. SAE Technical Paper. doi:10.4271/2019-01-0073
- Luo, F., Cui, H., and Dong, S. (2014). Transient Measuring Method for Injection Rate of Each Nozzle Hole Based on Spray Momentum Flux. *Fuel* 125, 20–29. doi:10.1016/j.fuel.2014.02.011

- Luo, T., Jiang, S., Moro, A., Wang, C., Zhou, L., and Luo, F. (2018). Measurement and Validation of Hole-To-Hole Fuel Injection Rate from a Diesel Injector. *Flow Meas. Instrum.* 61, 66–78. doi:10.1016/j.flowmeasinst.2018.03.014
- Manin, J., Kastengren, A., and Payri, R. (2012). Understanding the Acoustic Oscillations Observed in the Injection Rate of a Common-Rail Direct Injection Diesel Injector. *J. Eng. gas turbines power* 134, 122801. doi:10.1115/1.4007276
- Martínez-Martínez, S., de la Garza, O. A., García-Yera, M., Martínez-Carrillo, R., and Sánchez-Cruz, F. A. (2021). Hydraulic Interactions between Injection Events Using Multiple Injection Strategies and a Solenoid Diesel Injector. *Energies* 14, 3087. doi:10.3390/en14113087
- Matsuoka, S., Yokota, K., and Kamimoto, T. (1969). The Measurement of Injection Rate. *Proc. Institution Mech. Eng. Conf. Proc.* 184, 87–94. doi:10.1243/pime_conf_1969_184_323_02
- Meek, G., Williams, R., Thornton, D., Knapp, P., and Cosser, S. (2014). *F2E-ultra High Pressure Distributed Pump Common Rail System*. SAE Technical Paper. doi:10.4271/2014-01-1440
- Mohan, B., Yang, W., and Chou, S. k. (2013). Fuel Injection Strategies for Performance Improvement and Emissions Reduction in Compression Ignition Engines-A Review. *Renew. Sustain. Energy Rev.* 28, 664–676. doi:10.1016/j.rser.2013.08.051
- Mohan, B., Du, J., Sim, J., and Roberts, W. L. (2018). Hydraulic Characterization of High-Pressure Gasoline Multi-Hole Injector. *Flow Meas. Instrum.* 64, 133–141. doi:10.1016/j.flowmeasinst.2018.10.017
- Naber, J. D., and Siebers, D. L. (1996). *Effects of Gas Density and Vaporization on Penetration and Dispersion of Diesel Sprays*. SAE transactions, 82–111.
- Nehmer, D. A., and Reitz, R. D. (1994). *Measurement of the Effect of Injection Rate and Split Injections on Diesel Engine Soot and NOx Emissions*. SAE transactions, 1030–1041.
- Payri, R., García, J., Salvador, F., and Gimeno, J. (2005). Using Spray Momentum Flux Measurements to Understand the Influence of Diesel Nozzle Geometry on Spray Characteristics. *Fuel* 84, 551–561. doi:10.1016/j.fuel.2004.10.009
- Payri, R., Salvador, F. J., Martí-Aldaraví, P., and Martínez-López, J. (2012). Using One-Dimensional Modeling to Analyse the Influence of the Use of Biodiesels on the Dynamic Behavior of Solenoid-Operated Injectors in Common Rail Systems: Detailed Injection System Model. *Energy Convers. Manag.* 54, 90–99. doi:10.1016/j.enconman.2011.10.004
- Takamura, A., Ohta, T., Fukushima, S., and Kamimoto, T. (1992). *A Study on Precise Measurement of Diesel Fuel Injection Rate*. SAE Technical Paper. doi:10.4271/920630
- Tang, Q., Sampath, R., Sharma, P., Nyrenstedt, G., Al Ramadan, A., Houidi, M. B., et al. (2020). *Optical Study on the Fuel Spray Characteristics of the Four-Consecutive-Injections Strategy Used in High-Pressure Isobaric Combustion*. SAE Technical Paper. doi:10.4271/2020-01-1129
- Torelli, R., Som, S., Pei, Y., Zhang, Y., and Traver, M. (2017). Influence of Fuel Properties on Internal Nozzle Flow Development in a Multi-Hole Diesel Injector. *Fuel* 204, 171–184. doi:10.1016/j.fuel.2017.04.123
- Torelli, R., Matusik, K. E., Nelli, K. C., Kastengren, A. L., Fezzaa, K., Powell, C. F., et al. (2018). Evaluation of Shot-To-Shot In-Nozzle Flow Variations in a Heavy-Duty Diesel Injector Using Real Nozzle Geometry. *SAE Int. J. Fuels Lubr.* 11, 379–295. doi:10.4271/2018-01-0303
- Zeng, W., Xu, M., Zhang, M., Zhang, Y., and Cleary, D. J. (2012). Macroscopic Characteristics for Direct-Injection Multi-Hole Sprays Using Dimensionless Analysis. *Exp. Therm. fluid Sci.* 40, 81–92. doi:10.1016/j.expthermflusci.2012.02.003
- Zhang, Z., Liu, H., Yue, Z., Wu, Y., Kong, X., Zheng, Z., et al. (2022). Effects of Multiple Injection Strategies on Heavy-Duty Diesel Energy Distributions and Emissions under High Peak Combustion Pressures. *Front. Energy Res.* 430, 857077. doi:10.3389/fenrg.2022.857077
- Zhou, L.-Y., Dong, S.-F., Cui, H.-F., Wu, X.-W., Xue, F.-Y., and Luo, F.-Q. (2016). Measurements and Analyses on the Transient Discharge Coefficient of Each Nozzle Hole of Multi-Hole Diesel Injector. *Sensors Actuators A Phys.* 244, 198–205. doi:10.1016/j.sna.2016.04.017

Conflict of Interest: The authors declare that the research was conducted in the absence of any commercial or financial relationships that could be construed as a potential conflict of interest.

Publisher's Note: All claims expressed in this article are solely those of the authors and do not necessarily represent those of their affiliated organizations, or those of the publisher, the editors, and the reviewers. Any product that may be evaluated in this article, or claim that may be made by its manufacturer, is not guaranteed or endorsed by the publisher.

Copyright © 2022 Aljohani, Ben Houidi, Du, Dyuisenakhmetov, Mohan, AlRamadan and Roberts. This is an open-access article distributed under the terms of the Creative Commons Attribution License (CC BY). The use, distribution or reproduction in other forums is permitted, provided the original author(s) and the copyright owner(s) are credited and that the original publication in this journal is cited, in accordance with accepted academic practice. No use, distribution or reproduction is permitted which does not comply with these terms.